Br. J. exp. Path. (1986) 67, 865–877

Morphometry of the distribution of hydrostatic pulmonary oedema in dogs

René P. Michel, Sarkis Meterissian and Ronald S. Poulsen

The Lyman Duff Labs, and The McDonald Stewart, Biomedical Image Processing Laboratory, Department of Pathology, McGill University, and Royal Victoria Hospital, Montréal, Québec, Canada H3A 2B4

Received for publication 28 April 1986
Accepted for publication 18 July 1986

Summary. Light microscopic morphometry was utilized to examine the distribution of fluid in the interstitium around arteries, veins and within bronchovascular bundles in hydrostatic oedema, comparing it with previous control and permeability oedema experiments. Pulmonary artery wedge pressure was raised with fluid overload and an aortic balloon in five anaesthetized dogs to produce oedema (wet weight to dry weight ratios of 11.66 ± 0.84). Lung lobes were fixed by freeze-substitution at 20 mmHg airway pressure. Photomicrographs of arteries, veins and bronchovascular bundles were taken, and areas were digitized to obtain the following: (*a*) for arteries and veins, an oedema ratio = perivascular oedema cuff area/vessel area; (*b*) for bronchovascular bundles, T = total bundle area, A_1 = interstitial area around airways, B = airway (respiratory bronchiole, bronchiole, or bronchus) area, A_2 = periarterial interstitium, V = artery area. From these, oedema ratios were calculated as A_1/B and A_2/V. We found that (*a*) the oedema ratios were greater ($P < 0.01$) for arteries (1.18, $n = 675$) than veins (0·56, $n = 263$), and were greater for the larger vessels; (*b*) A_1 rose significantly ($P < 0.01$) only in bronchovascular bundles with bronchioles and bronchi, not in those with respiratory bronchioles; (*c*) A_2 increased from three- to 25-fold ($P < 0.01$) in all bundles; (*d*) A_1/B only increased in bundles with bronchi while A_2/V increased two- to six-fold in all bundles with oedema compared with controls. We conclude that these preferential patterns of distribution resemble those reported in permeability oedema, and may shed light on mechanisms of accumulation, and on the physiological effects of oedema on airways and vessels of the lung.

Keywords: pulmonary oedema, pulmonary artery, pulmonary vein, capillary permeability, pulmonary circulation, bronchus

When left atrial and pulmonary venous pressures are raised, either clinically in patients with left ventricular heart failure or experimentally, passive congestion occurs first, followed by the accumulation of interstitial oedema, and when the interstitial compartment is overloaded, by alveolar flooding (Staub *et al.* 1967; Staub 1974). Since the latter event is associated with deterioration in gas exchange, it is apparent that the interstitium plays an important role as a safety factor, particularly in hydrostatic

Correspondence: Dr René P. Michel, Lyman Duff Labs, Department of Pathology, Lyman Duff Medical Sciences Building, 3775 University St., Montréal, Québec, Canada H3A 2B4.

oedema, by acting as reservoir for the fluid: indeed Gee and Williams (1979) found that a substantial amount of fluid (2.6 ml/g dry blood-free lung) can accumulate in the interstitial space of isolated canine lung lobes filled with saline. Nonetheless, there are few studies which have quantified the relative distribution of oedema fluid in the different compartments of the interstitium, distribution which may explain the effects of oedema on lung mechanics and vascular resistance. Previously, we examined with morphometry the distribution of interstitial fluid in permeability oedema induced by α-naphthylthiourea (ANTU) and found more around arteries than veins and airways, and more around the larger vessels and airways (Michel *et al.* 1983, 1984). In the present study, we examined this distribution in hydrostatic oedema. Differences or similarities in the distribution and amount of interstitial oedema may shed some light on the mechanisms involved in its accumulation.

Materials and methods

A total of 13 adult mongrel dogs of either sex weighing 16–21 kg (mean 18 kg) were used for these experiments, including five dogs with oedema and eight control dogs. The latter were the same ones used in our previous studies (Michel *et al.* 1983; 1984). The animals were anaesthetized with pentobarbital sodium (25 mg/kg), intubated and allowed to breathe spontaneously. Femoral and cervical cutdowns were performed to introduce a Swan–Ganz catheter in the pulmonary arterial and pulmonary arterial wedge positions, a catheter in the femoral artery to monitor systemic arterial pressure, and two catheters for intravenous fluid administration. The pulmonary artery (p_{pa}) and pulmonary arterial wedge (p_{pw}) pressures were recorded at regular intervals on a Hewlett-Packard recorder. Arterial blood pO_2, pCO_2 and pH were measured in three of the oedema animals. A 6F Foley catheter was introduced via the carotid artery into the proximal aorta where it could be inflated to partially obstruct flow without lowering distal aortic pressure excessively and contribute to raising left atrial and pulmonary artery wedge pressure. Through a midline suprapubic incision, both ureters were ligated. After baseline measurements, the aortic balloon was inflated and warmed lactated Ringer's (20–25% body weight) was infused over 60 to 90 min to raise the p_{pw} to a peak of 30–40 mmHg. Chest radiographs were taken and with the arterial blood gases, used to monitor the development of the oedema. When the animals had moderately severe oedema, they were killed with an overdose of pentobarbital and the chest was opened. The lower lobes were removed after ligating the artery and vein, inflated to 20 mmHg airway pressure and frozen in liquid nitrogen; they were later cut with a band saw and sections taken from the mid-saggital slice and fixed by freeze-substitution in Carnoy's solution as previously described (Michel *et al.* 1983; 1984). Additional sections were also cut from the more medial parts of the lobes to find larger (>800 μm) arteries, veins and bronchovascular bundles. All tissues were processed for routine histology and paraffin sections were stained with haematoxylin and eosin. In addition, multiple samples were taken for measurements of wet weight to dry weight (W/D) ratios, as previously described (Michel *et al.* 1981); these were corrected for blood water with ^{51}Cr-labelled erythrocytes.

For the morphometry of the perivascular interstitial oedema, the microscopic slides were examined with a Leitz photomicroscope and arteries and veins from about 50 μm upward with their oedema cuff were photographed. Only intact vessels, clearly identifiable as artery or vein according to previously published criteria (Michel 1982), were chosen. The photographs were then projected on a Talos system 622B digitizing tablet interfaced to a Digital Equipment Corporation Vax 750 computer for data collection, storage and analysis. From the oedematous lungs, 675 arteries and 263 veins were studied. To quantify the amount of oedema around arteries and veins, an oedema ratio was

calculated, as previously described (Michel *et al.* 1983). To do this, the total area of the vessel with its interstitial oedema cuff was digitized; then, the area of the vessel was digitized at the external border of the media. The oedema ratio was computed as perivascular cuff area/vessel area. The diameter of the vessel was also measured and the oedema ratio results grouped according to vessel size categories for both arteries and veins. Appropriate corrections were made for shrinkage after fixation and embedding procedures. In addition to the oedema ratio, the absolute area of interstitial oedema cuff was calculated, expressed in square millimetres and also categorized by arteries and veins of different sizes.

To study the distribution of interstitial oedema within bronchovascular bundles, methods similar to those used with ANTU-induced oedema were employed, and compared with the same controls (Michel *et al.* 1984). From photographs of 183 bronchovascular bundles with oedema and 240 controls, five groups were examined: bundles with respiratory bronchioles, both separated and connected; bundles with bronchioles, separated and connected; and bundles with bronchi, which are always connected. To measure the areas in connected bronchovascular bundles, we traced four contours C_1 to C_4. These, and the areas obtained are illustrated in Fig. 1. C_1 was the outer contour of the total bundle; C_2 was the outer border of the interstitium around the airway (respiratory bronchiole, bronchiole or bronchus); C_3 was the airway contour traced at the subepithelial basement membrane; C_4 was the arterial contour, traced at the external border of the media. For respiratory bronchioles, the edges of the alveolar outpouchings were followed for both C_2 and C_3. From these traced contours, the following areas were computed (Fig. 1): T=area of C_1, was the total area of the bundle; B=area of C_3, was the airway area; V=area of C_4, was the arterial area; A_1=area of C_2-C_3, was the airway interstitial area; $A_2=C_1-(C_2+C_4)$ was the periarterial interstitial area. For the bundles with bronchi, the areas of the cartilaginous plates were also measured and subtracted from T and from A_1 (Michel *et al.* 1984).

For the separated bronchovascular bundles, a similar procedure was used (Fig. 2): C_1 to C_4 were analogous to those for the connected bundles except that C_1 was the periarterial interstitial cuff contour. The areas calculated were identical to the ones for connected bundles except that T=area C_1+C_2 and $A_2=C_1-C_4$. The data were computer analysed to yield absolute areas and oedema ratios for arteries (A_2/V) and airways (A_1/B) within bronchovascular bundles.

We also graded the amount of alveolar oedema with a semiquantitative system (Michel *et al.* 1983) ranging from 0 to 4: Grade 1 was 1 to 10% oedema, grade 2, 11 to 25%; grade 3, 26, to 50%; and grade 4, more than 50% oedema. This was done by estimating, out of the total alveolar surface area, the per cent area occupied by oedema fluid. We have used this system previously (Michel *et al.* 1981) and found it to be reproducible.

Results were expressed as means ±s.e. and statistics performed with the unpaired Student's *t*-test or with analysis of variance, with the Newman–Keuls test where required (Sokal & Rohlf, 1969). Values of $P<0.05$ were considered significant.

Results

The p_{pa} and p_{pw} rose from baseline values of 11.1±0.1 and 3.5±0.8 mmHg respectively to 40.4±2.7 and 36.4±1.4 mmHg at the end of fluid infusion. The arterial pO_2, in the three animals in which it was measured, fell from a baseline of 81.3±9.3 to 56.0±15.6 mmHg with oedema; pCO_2 did not vary (mean of 24.4 mmHg), while the pH fell slightly from a baseline of 7.42 to 7.35 with oedema. All the animals had moderate to severe oedema on the chest radiographs. The mean W/D ratios, corrected for blood water were 11.66±0.84 compared with 4.38±0.25 for the controls. When the chest

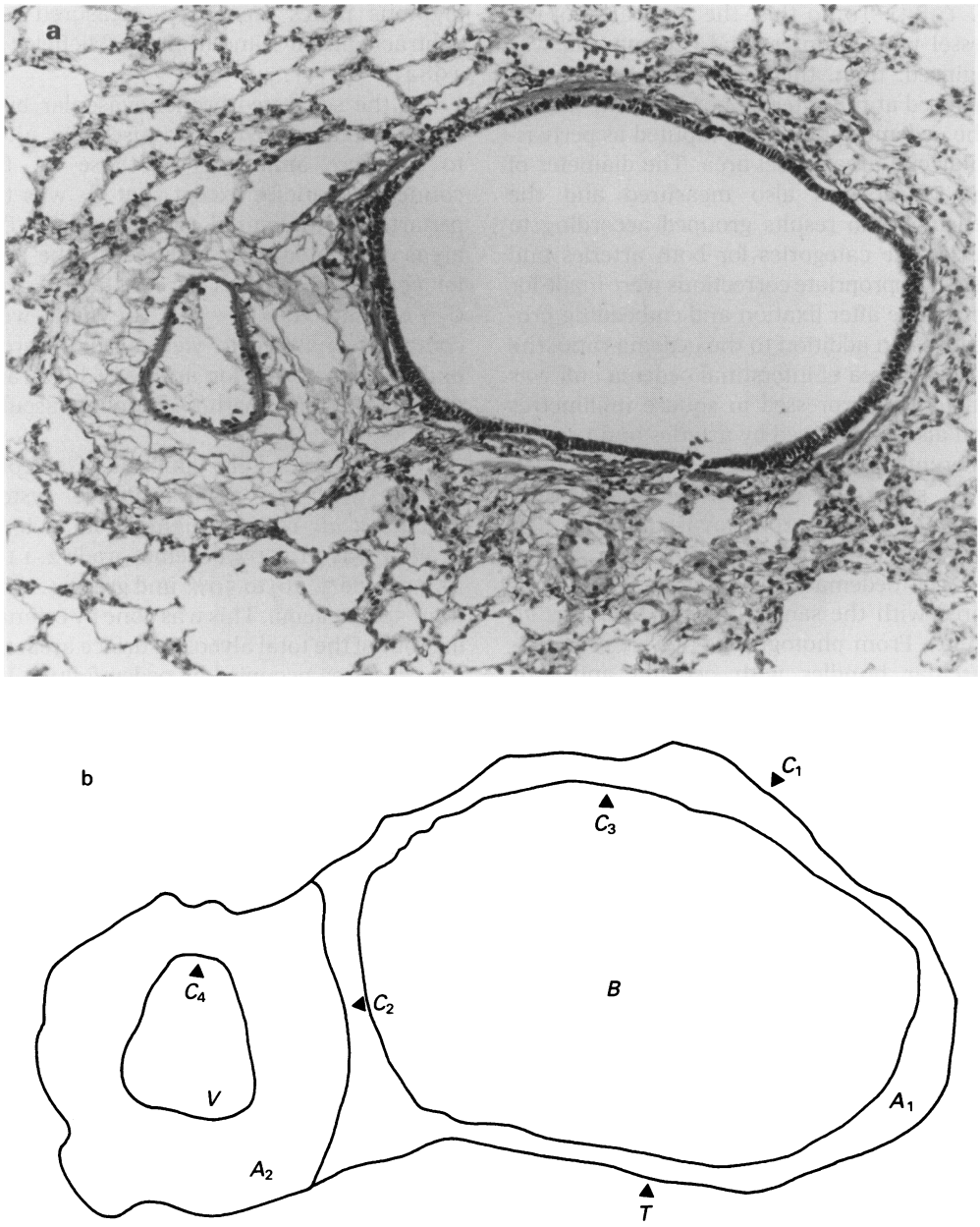

Fig. 1. *a*, Light photomicrograph from frozen lobe with oedema, of a connected bronchovascular bundle with a bronchiole (right) and an artery (left) with surrounding interstitial oedema cuff (H&E × 152, R-50a-4). *b*, Tracings of the contours: C_1 is the contour around the entire bundle, C_2 around the airway interstitium, C_3 around the airway and C_4 around the vessel. The corresponding areas obtained are *T*, *B*, *V*, A_1 and A_2 (see text for details).

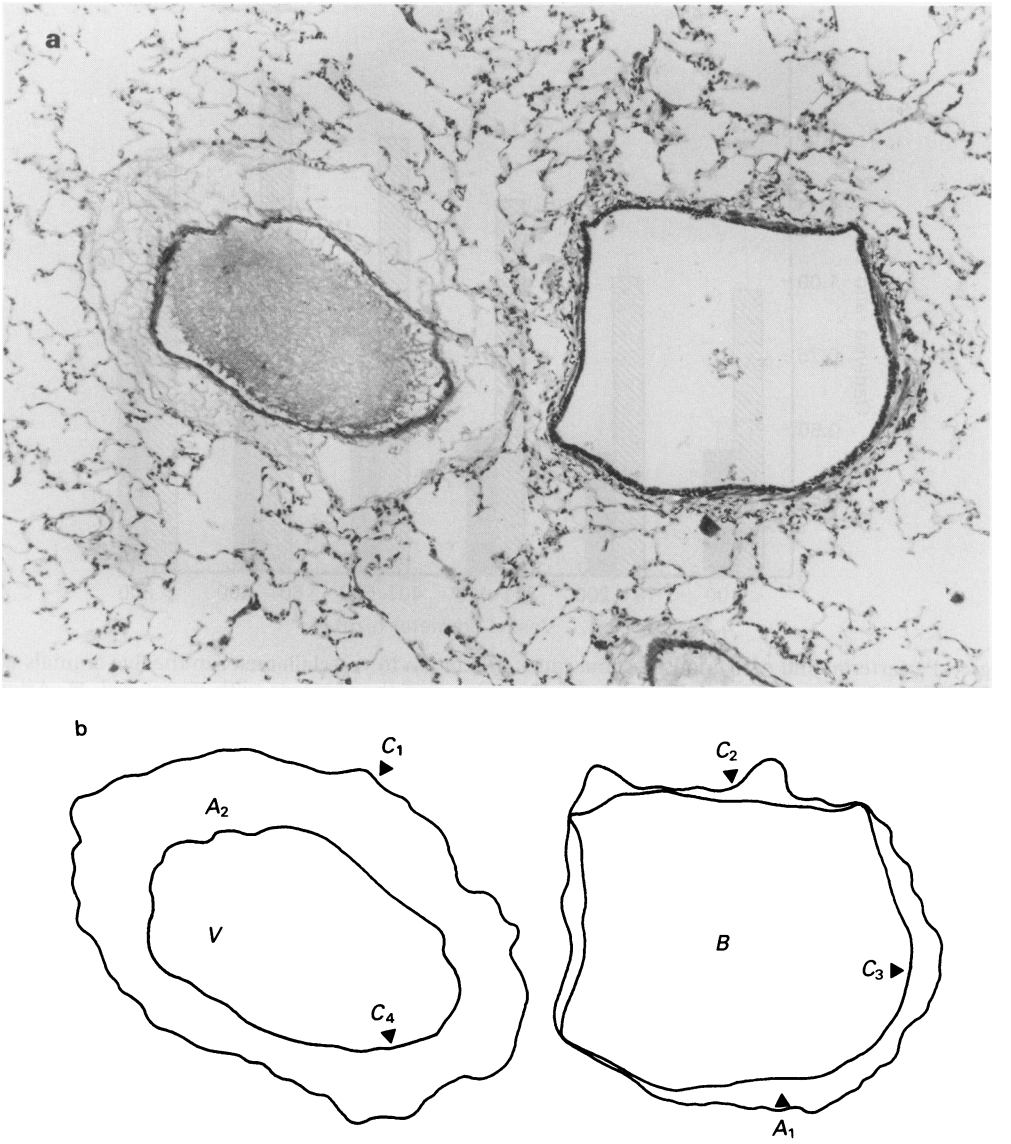

Fig. 2. *a*, Light photomicrograph of a separated bundle with a bronchiole (right) and an artery (left) (H&E × 96, R-50-0). *b*, Traced figure shows contours and areas analogous to those in Fig. 1*b*.

was opened post-mortem, fluid surrounded the hila of the lungs.

The results of the morphometry of the perivascular interstitial oedema are presented in Figs. 3 and 4. Comparison of the oedema ratios for arteries and veins of different size ranges showed significantly more oedema around arteries than veins ($P<0.01$), regardless of size. The mean oedema ratio was 1.18 for the arteries and 0.56 for the veins. In addition, for both arteries and veins, those over 400 μm diameter had significantly higher ratios than those under 400 μm ($P<0.01$). These results are similar to those for ANTU-induced oedema in relative distribution.

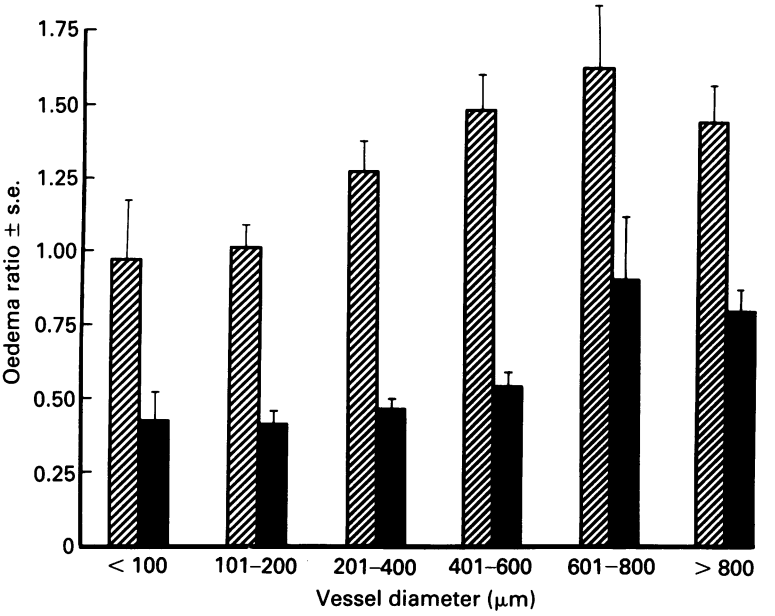

Fig. 3. Periarterial and perivenous oedema ratios in relation to vessel diameter in the five animals with hydrostatic oedema. Note smaller ratios for the veins and the increase with vessel size. ▨, Arteries ($n=675$); ■, veins ($n=263$).

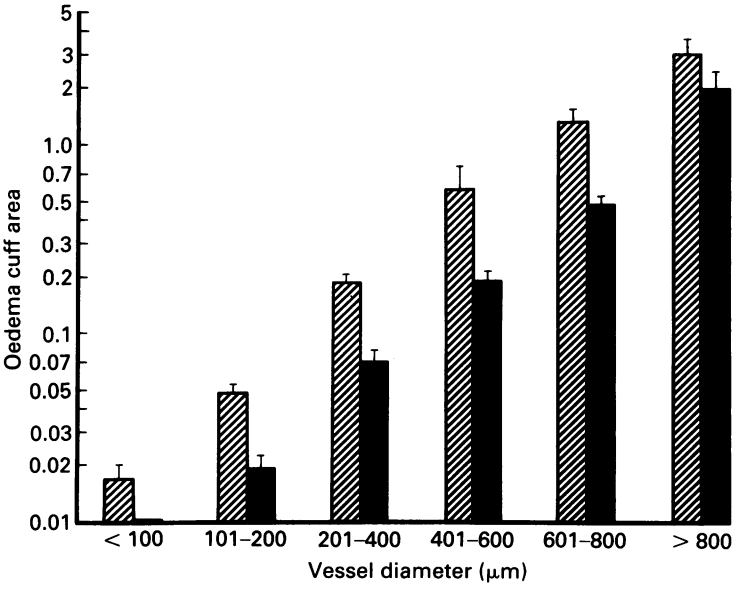

Fig. 4. Absolute area of oedema cuff for arteries and veins of different sizes. Note logarithmic scale and marked increase in cuff area with vessel size. ▨, Arteries; ■, veins.

The absolute amount of perivascular interstitial oedema was expressed in mm^2 as a function of vessel diameter. The results, plotted on a logarithmic scale in Fig. 4, show that with increasing vessel size, there is a rapid rise in the amount of interstitial cuff fluid around both arteries and veins. Statistical analysis of these data (Brown 1975; Michel *et al.* 1983) showed more oedema around arteries than veins ($P<0.01$).

We also examined the distribution of the total amount of perivascular oedema (Michel *et al.* 1983). The absolute oedema areas plotted in Fig. 4 indicate much more fluid collects around individual larger vessels, but do not take into account the fact there are many more small than large vessels. Therefore, using the data of Cumming *et al.* (1970) for arteries, and of Horsefield and Gordon (1981) for veins, to approximate the relative numbers of each categories of vessel size, we estimated the total amount of oedema at each level. These are plotted in Fig. 5 and reveal, although not amenable to statistical analysis, that there may be at least as much, if not more total oedema around the smaller vessels. It also suggests that overall, the periarterial interstitium holds more oedema than the perivenous interstitium.

The data for the distribution of interstitial oedema within bronchovascular bundles are presented in Figs. 6, 7, and 8, with the numbers of bundles in each group shown at the top. The diameters of the airways and arteries in each category of bronchovascular bundle are given in Table 1: for the respiratory bronchioles and bronchioles, they are clearly in the range of small airways, while those of the bronchi also include medium airways; as expected, the vessel diameters are smaller than those of the corresponding airways.

The total area of the bronchovascular bundles T (Figs. 6, 7, & 8) did not increase in separated bundles with respiratory bronchioles, the smallest of bundles, and rose, although not significantly, in all connected bundles with respiratory bronchioles and bronchioles. In the others, T increased significantly. Much of the increase in oedema is due, as was observed in ANTU-induced oedema, to an increase in the periarterial oedema area (A_2); this ranged from a three- to 25-fold increase for bundles with separated bronchioles and to a nearly 10-fold rise for bundles with bronchi. The interstitial area around airways (A_1) showed a significant ($P<0.01$) rise with oedema compared with control for bronchioles and bronchi, but not for respiratory bronchioles.

If we expressed, as done previously for ANTU oedema (Michel *et al.* 1984), A_2 as a

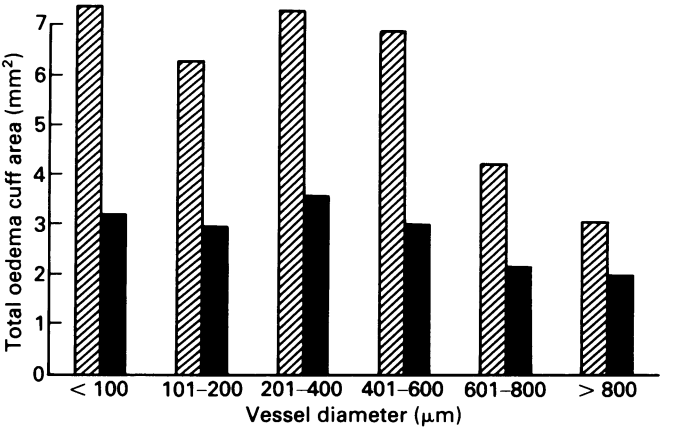

Fig. 5. Calculated estimate of total perivascular oedema cuff area for arteries and veins of different sizes, using data from Fig. 4 (see text for details). ▨, Arteries; ■, veins.

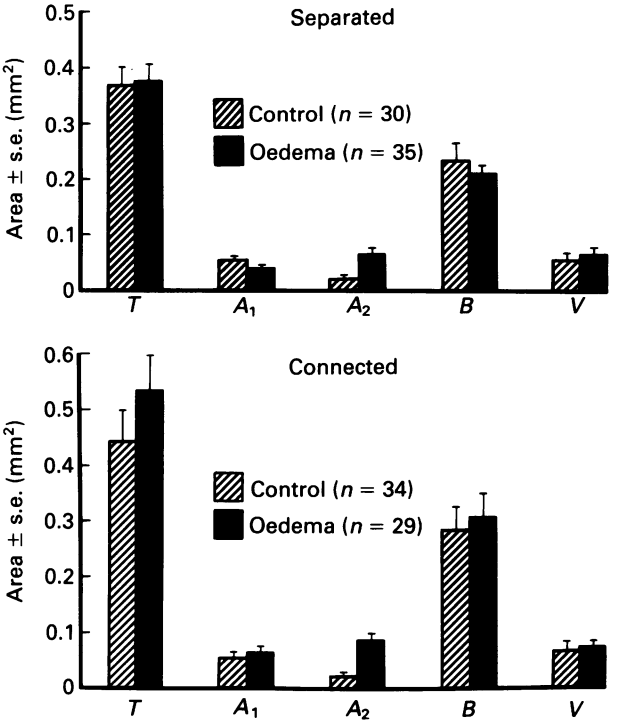

Fig. 6. Total area T, interstitial areas A_1, A_2, airway area B and vascular area V for bronchovascular bundles with respiratory bronchioles, both separated and connected, comparing oedema with previous controls. Note significant increase in A_2. n=no. of bundles.

per cent of bundle interstitium, i.e. of $T-(B+V)$, it accounted for 45 to 55% in oedema, compared with 10–35% in the controls. On the other hand, A_1, the interstitium around the airway, accounted for 45–55% of the interstitium after oedema, compared with 65–85% in the controls. Therefore the oedema preferentially accumulated around the arteries compared with the airways in all types of bronchovascular bundles.

Figure 9 shows the oedema ratios for airways (A_1/B) and arteries (A_2/V) for all bundles. In the case of the airways, only those with bronchi showed a significant rise ($P<0.01$), while for the arteries all increased from two- to six-fold in oedema compared with controls ($P<0.01$).

The values for alveolar oedema grades in these lobes were $0{\cdot}93\pm0{\cdot}11$. The oedema as seen by light microscopy in these experiments was less dark and pink compared with ANTU-induced oedema, but still easily recognizable.

Discussion

These experimental animals exhibited moderate to severe pulmonary oedema, as demonstrated by the fall in arterial pO_2, chest radiographs, post-mortem W/D ratios and morphology, which showed the presence of alveolar oedema. In this report, we performed morphometry only on frozen lobes, since we previously showed that instillation of fixative through the airways or its perfusion through the vasculature increased morphometric estimates of interstitial oedema (Michel *et al.* 1983). Similar effects of these fixation methods were demonstrated in

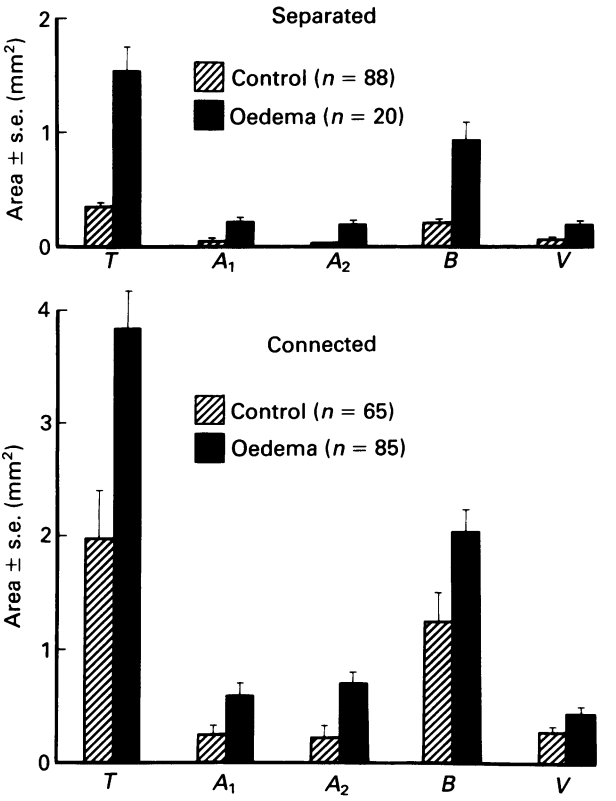

Fig. 7. Same areas as in Fig. 6 for bundles with bronchioles. Both A_1 and A_2 increase.

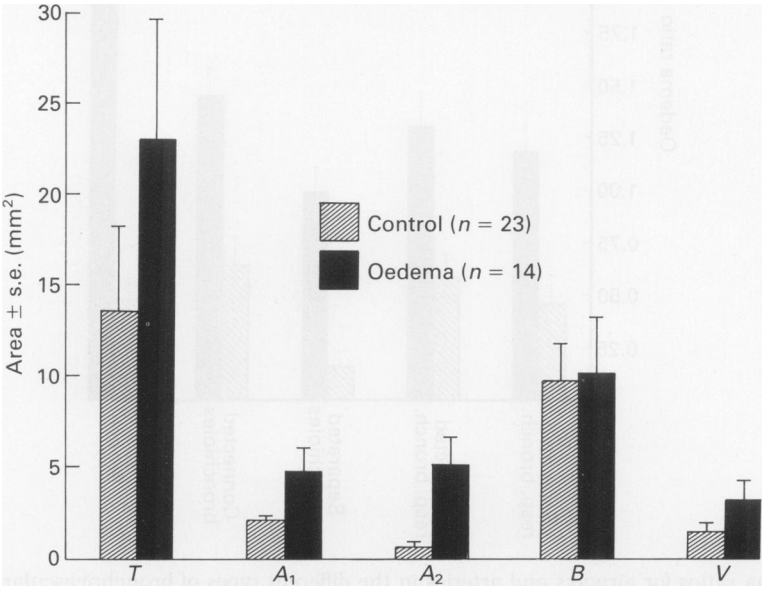

Fig. 8. Same areas as in Fig. 6 for bundles with bronchi (all connected). A_2 increases substantially more than A_1 compared with controls.

Table 1. Diameters of airways and vessels in bronchovascular bundles

	Respiratory bronchioles		Bronchioles		Bronchi
	Separated	Connected	Separated	Connected	Connected
Airways (mm ± s.e.)					
Control	0.38±0.02	0.47±0.07	0.41±0.02	0.88±0.09	2.32±0.30
Oedema	0.40±0.02	0.47±0.03	0.80±0.06	1.14±0.12	2.31±0.36
Vessels (mm ± s.e.)					
Control	0.17±0.01	0.17±0.02	0.19±0.01	0.27±0.04	0.75±0.10
Oedema	0.20±0.01	0.20±0.01	0.34±0.03	0.46±0.05	1.32±0.19

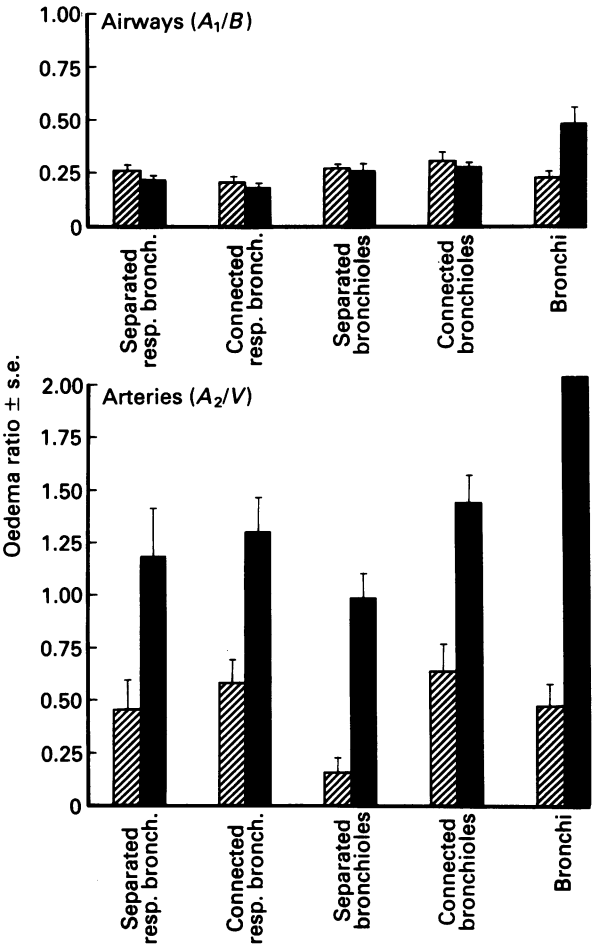

Fig. 9. Oedema ratios for airways and arteries in the different types of bronchovascular bundle. A_2/V increases markedly in all bundles, while A_1/B only does so in those with bronchi. ■, Control; ■, oedema.

a study of microvascular permeability to the tracer dextran (Michel 1985).

This study was designed to investigate the accumulation of oedema in the interstitial compartments surrounding the larger vessels and the airways, rather than the alveolar septal and pericapillary interstitium. De Fouw (1982) investigated the latter with ultrastructural morphometry and found that the thickness of the air-blood barrier was increased with hydrostatic and oncotic oedema in isolated lobes.

The principal results of this study were that, in hydrostatic oedema induced by an aortic balloon and fluid overload in intact, close-chested anaesthetized dogs, the interstitial fluid accumulated preferentially around arteries compared with veins and around larger compared with smaller vessels; this occurred whether oedema ratios (Fig. 3) or absolute amounts of oedema (Fig. 4) were looked at. Within bronchovascular bundles, substantially more fluid was found around arteries than airways; indeed around the smaller airways (respiratory bronchioles), A_1 did not increase compared with controls, while for both respiratory bronchioles and bronchioles, oedema ratios were not significantly higher than controls (Fig. 9). The increase in A_1 for bundles with bronchioles (Fig. 7) may be due to a sampling of somewhat larger airways in the oedema group, since these had larger B areas. The oedema ratio, which takes this into account, suggests there is no more oedema around bronchioles than around respiratory bronchioles. Paucity of fluid accumulation around small airways is supported by a recent study (Michel 1985) in which, in ANTU-induced oedema, dextran was injected just before killing: under these circumstances, while the tracer entered the interstitium around smaller vessels, lymphatics and alveoli, much less was found around airways in larger bronchovascular bundles, and none visualized around small airways.

The finding of minimal fluid around smaller airways may have implications in the mechanism of alveolar flooding in hydrostatic oedema. Indeed, the notion that it occurs through alveolar epithelial intercellular junctions has been questioned: Gee and Staub (1977) and Staub (1983) proposed, based on experimental studies of protein movement from alveoli to interstitium, that in severe oedema, liquid overflows from the peribronchovascular connective tissue into the lumen of small airways via high conductance pathways and fills alveoli in a retrograde manner. This theory of alveolar flooding (Staub 1983) would then, in light of the findings in this and previous studies (Michel *et al.* 1984) occur at a level more proximal than previously thought, an idea also supported by the recent study of Mason and Effros (1983) on *in situ* perfused rabbit lungs.

Our present findings are similar to those we reported in ANTU-induced oedema (Michel *et al.* 1983, 1984), with a preponderance of fluid around arteries, around larger vessels and around arteries compared with airways. This suggests that the factors responsible for the pattern of interstitial oedema accumulation may be independent of the aetiology and type of oedema, i.e. permeability or hydrostatic; these factors, discussed previously (Michel *et al.* 1983, 1984) include the mechanical properties of anatomic spaces, the amount and distribution of connective tissue and gradients of interstitial pressures. Another possible factor which has not been mentioned is whether the site of filtration has bearing on its accumulation: Whayne and Severinghaus (1968) suggested that the periarterial cuffs could originate from direct transarterial leakage; a similar mechanism could occur on the venous side. The plausibility of this mechanism has been demonstrated by physiological studies of extra-alveolar vessel leakage (Albert *et al.* 1983) as well as by morphological tracer studies (Yoneda 1980; Michel 1985). Whether this contribution is significant in the pattern of interstitial fluid accumulation remains to be tested.

If the relative distribution of fluid was similar in ANTU-induced (Michel *et al.* 1983,

1984) and in hydrostatic oedema, the amount of oedema differed. Indeed, the oedema ratios of vessels and the areas of oedema were less with hydrostatic oedema, although the amounts of alveolar oedema did not differ significantly. One might have expected, on the basis of the W/D ratios, more fluid with hydrostatic (W/D ratio of 11.66) than with permeability (W/D ratio of 7.82) oedema. However, these W/D ratios cannot be compared directly since in permeability oedema, the dry weight increases due to the greater amount of filtered protein (Staub 1974; Julien *et al.* 1984). If we used a correction factor analogous to the one proposed by Julien *et al.* (1984), the W/D ratios after ANTU would increase from 7.82 to 10.09, closer to the 11.66 of the hydrostatic oedema experiments; furthermore the W/D of 11.66 may still be an overestimate since we used larger volumes of fluid than Julien *et al.* (personal communication) and our dry weight may have been lower than normal due to the washout of proteins. Another possible explanation may be time-related: indeed with ANTU, the oedema developed over 5–7 h, allowing plenty of time for the fluid to enter the sequestered cuff spaces (Gee & Havill 1980); with fluid overload however, a short time elapsed before fixation of the lobes, and relatively more fluid may have been present in interalveolar septa and around very small vessels, which could not be assessed in our study. A third explanation for the quantitative differences between ANTU and hydrostatic oedema may be the higher intravascular pressure during the latter: this could lower the interdependence between airways, arteries and the parenchyma, as demonstrated by Parker *et al.* (1981), and result in smaller amounts of interstitial fluid accumulating within bronchovascular bundles and around vessels.

In a recent study, Montaner *et al.* (1984) compared hydrostatic and oleic acid oedema, and found more alveolar flooding and less interstitial oedema with oleic acid. While these results appear to contradict ours, the differences in the greater severity (with haemorrhage) and rapidity of onset of oedema produced by oleic acid (Ehrhart & Hofman 1981; Malo *et al.* 1984) compared with ANTU (Gee & Havill 1980), probably account for the differences. Indeed, in a recent study of nitrogen dioxide-induced oedema, we demonstrated preferential alveolar flooding with minimal or absent interstitial cuffing (Vassilyadi & Michel 1985).

In summary, our data show that in hydrostatic, as in permeability oedema, a characteristic pattern of interstitial oedema fluid accumulation emerges which is intimately related to known variables of lung physiology and may be related to other as yet unexplored mechanisms. Furthermore, these patterns of interstitial oedema fluid accumulation may help to elucidate the mechanisms of alteration of respiratory mechanics (e.g., lung and airway resistance) and vascular resistance observed with lung oedema.

Acknowledgements

This research was supported by Medical Research Council of Canada Grant MA-7727, and the Québec Lung Association. The authors thank Mr T. Smith for technical assistance and Mrs S. Totilo for secretarial help in preparation of the manuscript.

References

ALBERT R.K., LAKSHMINARAYAN S., CHARAN N.B., KIRK W. & BUTLER J. (1983) Extra-alveolar vessel contribution to hydrostatic pulmonary oedema in *in situ* dog lungs. *J. Appl. Physiol. Respirat. Environ. Exercise Physiol.* **54**, 1010–1017.

BROWN M.B. (1975) A method for combining non-independent one-sided tests of significance. *Biometrics*, **31**, 987–992.

CUMMING G., HARDING L.K., HORSFIELD K., PROWSE K., SINGHAL S.S. & WOLDENBERG M. (1970) Morphological aspects of the pulmonary circulation and of the airways. In *Fluid Dynamics of Blood Circulation and Respiratory Flow*, Vol. 65, NATO Advisory Group for Aerospace Research and Development, conference proceedings. pp. 23–30.

DE FOUW, D.O. (1982) Ultrastructure of the pulmonary alveolar septa after hemodynamic oedema. *Ann. NY. Acad. Sci.* **384**, 44–53.

EHRHART I.C. & HOFMAN W.F. (1981) Oleic acid dose-related oedema in isolated canine lung perfused at constant pressure. *J. Appl. Physiol. Respirat. Environ. Exercise Physiol.* **50**, 1115–1120.

GEE M.H. & HAVILL A.M. (1980) The relationship between pulmonary perivascular cuff fluid and lung lymph in dogs with oedema. *Microvasc. Res.* **19**, 209–216.

GEE M.H. & STAUB N.C. (1977) Role of bulk fluid flow in protein permeability of the dog lung alveolar membrane. *J. Appl. Physiol.* **42**, 144–149.

GEE M.H. & WILLIAMS D.O. (1979) Effect of lung inflation on perivascular cuff fluid volume in isolated dog lung lobes. *Microvasc. Res.* **17**, 192–201.

HORSFIELD K. & GORDON W.I. (1981) Morphometry of pulmonary veins in man. *Lung.* **159**, 211–218.

JULIEN M., FLICK, M.R., HOEFFEL M.J. & MURRAY J.F. (1984) Accurate reference measurement for postmortem lung water. *J. Appl. Physiol. Respirat. Environ. Exercise Physiol.* **56**, 248–253.

MALO J., ALI J. & WOOD L.D.H. (1984) How does positive end-expiratory pressure reduce intrapulmonary shunt in canine pulmonary oedema? *J. Appl. Physiol. Respirat. Environ. Exercise Physiol.* **57**, 1002–1010.

MASON G.R. & EFFROS R.M. (1983) Flow of oedema fluid into pulmonary airways. *J. Appl. Physiol. Respirat. Environ. Exercise Physiol.* **55**, 1262–1268.

MICHEL R.P. (1982) Arteries and veins of the normal dog lung: qualitative and quantitative structural differences. *Am. J. Anat.* **164**, 227–241.

MICHEL R.P. (1985) Lung microvascular permeability to dextran in alpha-naphthylthiourea-induced oedema: Sites of filtration, patterns of accumulation and effects of fixation. *Am. J. Pathol.* **119**, 474–484.

MICHEL R.P., HAKIM T.S., SMITH T.T. & POULSEN R.S. (1983)Quantitative morphology of permeability lung oedema in dogs induced by alpha-naphthylthiourea. *Lab. Invest.* **49**, 412–419.

MICHEL R.P., LAFORTE M. & HOGG J.C. (1981) Physiology and morphology of pulmonary microvascular injury with shock and reinfusion *J. Appl. Physiol. Respirat. Environ. Exercise Physiol.* **50**, 1227–1235.

MICHEL R.P., SMITH T.T. POULSEN R.S. (1984) Distribution of fluid in bronchovascular bundles with permeability lung oedema induced by alpha-naphthylthiourea in dogs. A morphometric study. *Lab. Invest.* **51**, 97–103.

MONTANER J.S.G., WIGGS B., WALKER D.C. & HOGG J.C. (1984) The distribution of extravascular lung water (EVLW) in high (HPPE) and low pressure pulmonary edema (LPPE) (abstr). *Am. Rev. Resp. Dis.* **129**, A 346.

PARKER J.C., ALLISON R.C. & TAYLOR A.E. (1981) Edema affects intra-alveolar fluid pressures and interdependence in dog lungs. *J. Appl. Physiol. Respirat. Environ. Exercise Physiol.* **51**, 911–921.

RUTILI G., KVIETYS P., MARTIN D., PARKER J.C. & TAYLOR A.E. (1982) Increased pulmonary microvascular permeability induced by alpha-naphthylthiourea. *J. Appl. Physiol. Respirat. Environ. Exercise Physiol.* **52**, 1316–1323.

SOKAL R.R. & ROHLF F.J. (1969) *Biometry. The Principles and Practice of Statistics in Biological Research.* San Francisco: W.H. Freeman. pp. 1–776.

STAUB N.C. (1974) Pulmonary edema. *Physiol. Rev.* **54**, 678–811.

STAUB N.C. (1983) Alveolar flooding and clearance. *Am. Rev. Resp. Dis.* **127**, S44–S51.

STAUB N.C., NAGANO H. & PEARCE M.L. (1967) Pulmonary edema in dogs, especially the sequence of fluid accumulation in lungs. *J. Appl. Physiol.* **22**, 227–240.

VASSILYADI M. & MICHEL R.P. (1985) Sequence of fluid accumulation in nitrogen dioxide (NO_2)-induced lung edema in dogs: a morphometric study (abstr). *Physiologist, 28*, 350.

WHAYNE T.F. JR. & SEVERINGHAUS J.W. (1968) Experimental hypoxic pulmonary edema in the rat. *J. Appl. Physiol.* **25**, 729–732.

YONEDA K. (1980) Anatomic pathway of fluid leakage in fluid-overloaded pulmonary edema in mice. *Am. J. Pathol.* **101**, 7–16.